water

MDPI

Article

Topographical Analysis of the 2013 Typhoon Haiyan Storm Surge Flooding by Combining the JMA Storm Surge Model and the FLO-2D Flood Inundation Model

Lea Dasallas [1] and Seungsoo Lee [2,*]

[1] Department of Agricultural & Rural Eng., Chungnam National University, Daejeon 34134, Korea; leadasallas@gmail.com
[2] Climate Prediction Team, APEC Climate Center, Busan 48058, Korea
* Correspondence: seungsoo_lee@apcc21.org; Tel.: +82-51-745-3948

Received: 26 November 2018; Accepted: 8 January 2019; Published: 15 January 2019

Abstract: The floods associated with the effects of an incoming tropical cyclone have an immense effect in the Philippines, especially with respect to agriculture, industry, livelihood, and public safety. Knowledge of how such storm surge flooding can affect the community is therefore of great importance. In this study, the mechanisms behind Typhoon Haiyan's anomalous storm surge flooding in 2013, which resulted in more than 6300 casualties and 2.86 billion USD worth of damage in the Philippines, were investigated. The Japan Meteorological Agency (JMA) storm surge model and the FLO-2D flood model were used to simulate Typhoon Haiyan's storm surge height and the extent of inundation, respectively. The storm surge input data were obtained from JMA typhoon data, and the digital terrain models used were gathered from the airborne interferometric synthetic aperture radar data. The model's accuracy was also validated using field validation data of the extent of the observed storm surge in affected coastal areas. Topographical analysis of the inundated regions showed the effects of coastal shape, elevation, and position relative to the typhoon's approach angle on storm surge flow depth and velocity. Storm surge maximum velocity appears to increase as the fluid flows to an increasingly elevated area. Observing fluid velocity in a coastal area with uniform storm surge discharge from all directions also showed that flow velocity tends to increase at the center. Greater flood depths were experienced in areas with lower coastal elevation and not directly located at the coast, compared to higher elevation coastal areas. Greater extents of storm surge flooding are expected in coastal areas that have a concave shape, as fluid is more likely to be dispersed when hitting a convex coast. Extents are likewise observed to be greater in coastal regions that are located perpendicular to the direction of the typhoon. The research also validated the option of using a combination of typhoon and flood models to simulate the inundation flooding caused by extreme weather events.

Keywords: storm surge model; flood model; extreme weather events; topographical characteristics; inundation extent; inundation depth

1. Introduction

The natural hazards generated by a tropical cyclone impose significant threats, especially to coastal communities. These hazards, such as rainfall-induced flooding and landslides, and the storm surges generated by the strong winds, have been known to result in substantial loss of life and damage to properties in the Philippines. One particular cyclone, Typhoon Haiyan in 2013, affected 16 million people and resulted in about 6300 deaths, making it the deadliest typhoon to hit the country in recent history [1]. The number of casualties was primarily associated with the anomalous storm surge flooding generated by the typhoon [2].

However, modeling storm surges is not as common and well known as flood and debris flow modeling. This is mainly due to the rarity of storm-surge-related hazards compared with the hazards associated with flooding events. In recent years, however, several storm surge models have been developed by atmospheric and coastal researchers. These storm surge models include the Sea Lake and Overland Surges from Hurricanes model by the National Oceanic and Atmospheric Administration (NOAA) and National Hurricane Center [3,4], the Mike21 and Mike Flood models [5] developed by the DHI Water and Environment Corporation, the Delft3D coastal surge model [6] by Deltares, and the Japan Meteorological Agency (JMA) storm surge model [7] from the Japan Meteorological Agency.

The 2013 Typhoon Haiyan storm surge has been evaluated by several researchers using different models, these topics include: ensemble forecasting [8,9], boulder and sediment transport [10,11], storm surge simulations [2,12–14], local amplifications [15], and spatial variation of damages [16]. Most of these research efforts focused on simulation of the storm surge of the event, but very few of those presented the inland flooding generated by the storm surge. [2] presented a simulated storm surge inundation and field validation results using the same models as in the present study. However, the paper showed only one affected area (Tacloban City) and focused more on the social aspects of the event rather than the scientific factors behind.

To determine the factors leading to the extreme flooding caused by the Haiyan storm surge, it is important to analyze the meteorological and geographical conditions present during the event that caused the aggravation of storm surge flooding. In other words, the topographical characteristics of the areas that made them more susceptible to inundation compared with the other areas that experienced the same typhoon intensity must be considered.

The objective of this paper is to analyze the geographical characteristics of the most affected areas during the typhoon storm surge event. The motivation in doing so is the lack of related literature discussing the vulnerability of coastal areas to storm surges as a result of their topographical characteristics. These analyses include the effects of coastal shape, elevation, the position relative to the typhoon's angle of approach to the storm surge depth, extent, and flow velocity. However, the meteorological conditions that instigated such intensity, which in turn caused the anomalous storm surge, are not covered in this research, but will be discussed in greater detail in our future research.

This research utilized the JMA storm surge model for storm surge simulation. The JMA model uses a two-dimensional shallow water equation and is used to model typhoon-induced storm surges that form in the northwestern Pacific basin. While there are a number of storm surge models that can simulate the same effect with much finer resolution, the JMA model was chosen for this research due to its higher advantage in terms of computational speed. The JMA model's capability of simulating reliable storm surge timeseries with less computational time is ideal for simulating larger domains, while not losing the objective of the research. The inland storm surge flooding, however, which the model lacks, was supplemented using the FLO2D flood model, a flood routing model that simulates overland flow over complex topography. In this study, field validation data are also provided to show the accuracy of the models used. The structure of the paper is arranged as follows: Section 2 describes the data and the data sources used, as well as the governing equations and procedures behind the storm surge and flood models. Section 3 shows the results of the inundation model, comparison with field observations, and the analysis of the storm surge depth and velocity in response to the difference in topography. Finally, Section 4 provides a summary and final conclusion for the research.

2. Data and Methods

To simulate the storm surge flooding generated by Typhoon Haiyan 2013, the research utilized the tropical cyclone best track data [17] obtained from the JMA typhoon archive.

The study domain elevation and topographical characteristics were represented using the airborne interferometric synthetic aperture radar-derived digital terrain model (DTM) with a 5 m spatial resolution. The bathymetric data used for the domain were the 2 min Global Gridded Elevation data (ETOPO2) gathered from the NOAA.

To simulate the Haiyan-induced storm surge height and the extent of inundation for the most affected coastal areas, the JMA storm surge model and the FLO-2D flood routing model were used together.

2.1. Storm Surge Model (JMA)

To simulate Typhoon Haiyan's storm surge height, the JMA storm surge model, a two-dimensional numerical model that uses a vertically integrated momentum equation and a continuity equation [7], was employed. This model computes storm surge height caused by wind and inverted barometric effect, and its inputs are the typhoon track and bathymetric data.

The storm surge model's governing equations are as follows:

$$\frac{\partial U}{\partial t} - fV = -g(D+\eta)\frac{\partial(\eta-\eta_0)}{\partial x} + \frac{\tau_{sx}}{\rho} - \frac{\tau_{bx}}{\rho} \tag{1}$$

$$\frac{\partial V}{\partial t} - fU = -g(D+\eta)\frac{\partial(\eta-\eta_0)}{\partial y} + \frac{\tau_{sy}}{\rho} - \frac{\tau_{by}}{\rho} \tag{2}$$

$$\frac{\partial \eta}{\partial t} + \frac{\partial U}{\partial x} + \frac{\partial V}{\partial y} = 0 \tag{3}$$

where U and V are mass fluxes in the x and y directions, defined as

$$U \equiv \int_{-D}^{\eta} u dz \tag{4}$$

$$V \equiv \int_{-D}^{\eta} v dz \tag{5}$$

where u and v are the x and y direction velocities, z is the vertical length, D is the water depth below mean sea level, η is the surface elevation, η_0 is the water column height corresponding to the inverse barometer effect, f is the Coriolis parameter, g is the acceleration due to gravity, ρ is water density, τ_{sx} and τ_{sy} are the x and y components of wind stress on the sea surface, and τ_{bx} τ_{by} are the x and y components of bottom friction stress. Wind stresses are expressed as

$$\tau_{(sx,sy)} = c_d \rho_a W(u_w v_w) \tag{6}$$

where c_d is the drag coefficient, ρ_a is the air density, $W \equiv \sqrt{u_w^2 + v_w^2}$ is the wind speed, and (u_w, v_w) is the wind velocity. The drag coefficient is set using the results of [18] and [19]:

$$c_d = \begin{cases} (0.63 + 0.066W) \times 10^{-3} & \text{if } (W < 25 \text{ m/s}) \\ (2.28 + 0.033(W-25)) \times 10^{-3} & \text{if } (W \geq 25 \text{ m/s}) \end{cases} \tag{7}$$

We solved these equations by numerical integration, using the explicit finite difference method. For more details on the JMA storm surge model, refer to [20].

Typhoon track data were composed of meteorological descriptions of Typhoon Haiyan, such as its formation and dissipation dates, eye center location (latitude and longitude), maximum sustained wind speed in kts, and central pressure in hPa. Using these input data, which are essential for running the JMA storm surge model, we ran a storm surge simulation using three domains, as shown in Figure 1:

(1) 114° E–135° E, 5° N–25° N; (2) 118° E–128° E, 8° N–24° N; and (3) 115° E–160° E, 5° N–25° N. Domain 1 covers the storm surge rise and fall over the Philippine Area of Responsibility (region in the northwestern pacific where the Philippines' national meteorological agency monitors significant weather disturbances), domain 2 identifies the regions that recorded the highest sea level rise during Typhoon Haiyan, and domain 3 shows Typhoon Haiyan's life span from cyclogenesis to dissipation.

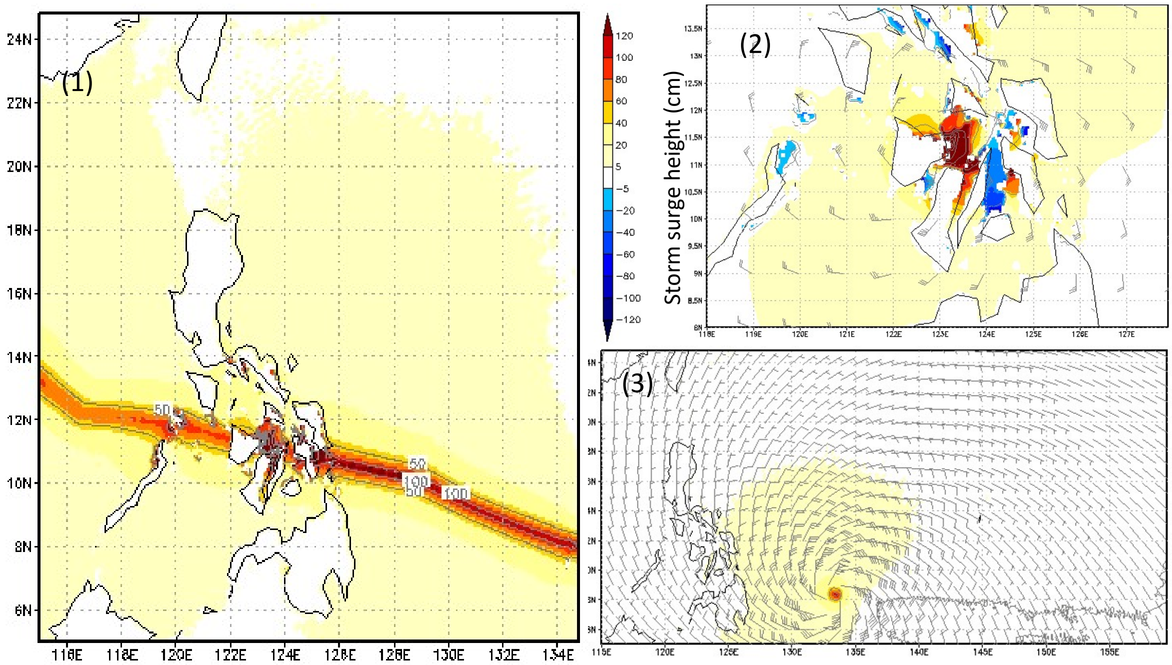

Figure 1. Domains used for simulating the storm surge height using JMA (Japan Meteorological Agency) storm surge model.

At the sea–land interface, the normal component of velocity is zero. At open boundaries, the sea surface elevation is given by the inverted barometer effect; a gravity wave radiation condition was used in this study. Tides can be simulated but are excluded, since the major object of this simulation is for surge heights.

Our simulations produced storm surge height time series for each domain. We modified the storm surge height to incorporate astronomical tides computed using WxTide, a Windows-based tide and current prediction program. We determined the coastal provinces targeted for flood simulation from the results of our JMA storm surge simulation. The storm tide (storm surge depth + astronomical tide) time series from the JMA model was used as the input file for our storm surge inundation simulation.

The JMA storm surge model simulation identified the provinces of Iloilo, Leyte, Palawan, Samar, and Eastern Samar as having experienced the highest storm surge during Typhoon Haiyan. The location of the provinces can be viewed in the coastal inundation model results. The greatest estimated storm surge height reached about 3.9 m in Batad, Iloilo (Figure 2). We then used the catchments of these provinces for our flood inundation simulation.

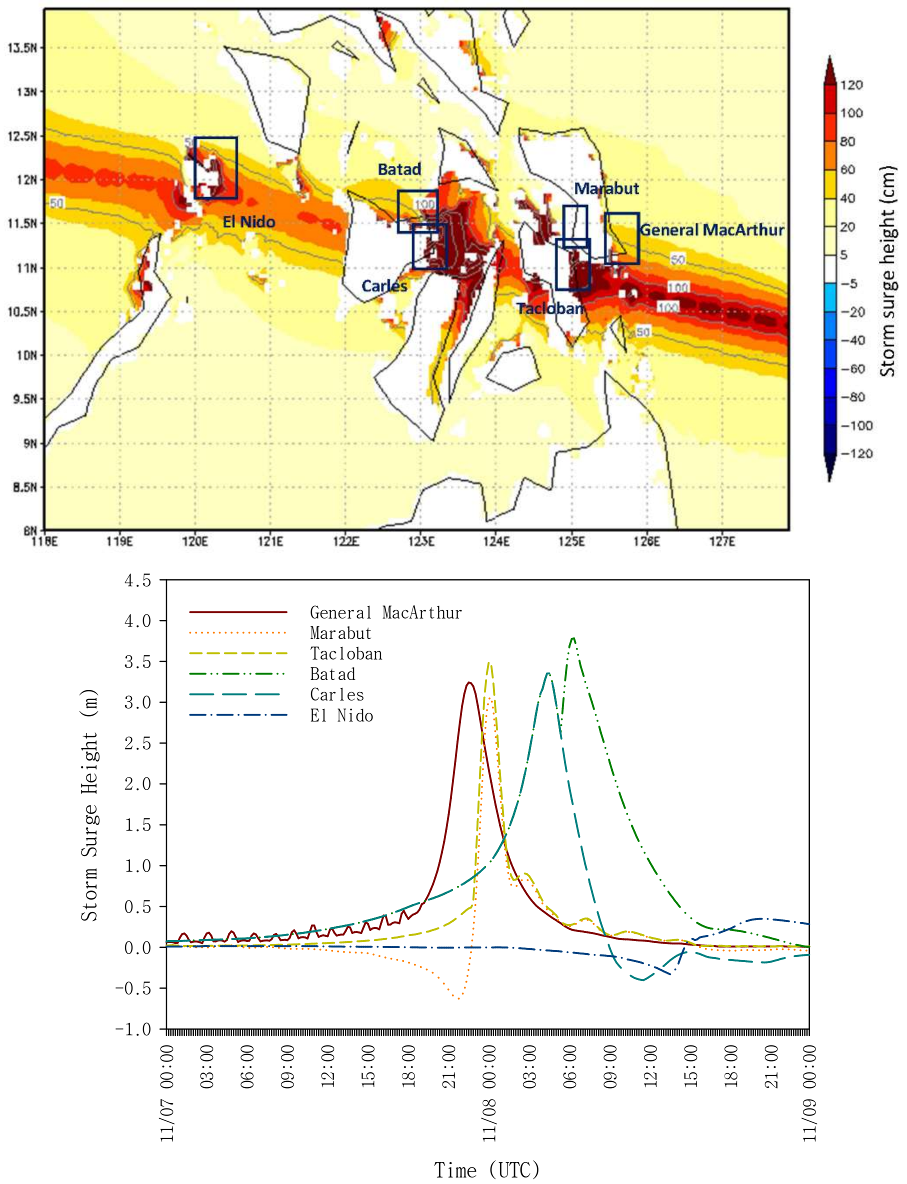

Figure 2. Most affected coastal areas (**upper panel**) and their respective simulated storm surge time series results (**lower panel**).

2.2. Coastal Inundation Model

One of the JMA storm surge model's limitations is that it does not simulate storm surge inundation. The extent of storm surge flooding predictions is crucial for pre-emptive evacuation and long-term urban planning. Storm surge inundation maps were employed in this study using the FLO2D model, a flood routing model that simulates channel, overland, and street flow over complex topography. We chose the FLO2D model to conduct our flood simulation because of its compatibility with the JMA storm surge model. The FLO2D model's limitations, such as the absence of wave coefficients and receding parameters, were not deemed significant enough to drastically affect this study's objective and results. FLO2D's governing equations are as follows:

$$\frac{\partial h}{\partial t} + \frac{\partial hV}{\partial x} = r_e \tag{8}$$

$$S_f = S_0 - \frac{\partial h}{\partial x} - \frac{V}{g} - \frac{\partial V}{\partial x} - \frac{1}{g}\frac{\partial V}{\partial t} \tag{9}$$

where t represents time; h is the flow depth; hV is the depth-averaged velocity in one of eight flow directions; x, r_e is the excess rainfall intensity; S_f is the friction slope component based on Manning's equation; S_0 is the bed slope pressure gradient; and g is the acceleration due to gravity. This equation represents a one-dimensional, depth-averaged channel flow. For the floodplain, although FLO-2D is a multi-direction flow model, FLO-2D's equations of motion are applied by computing average flow velocity across a grid element boundary one direction at a time [21].

The catchments to simulate for flooding were chosen using the previous storm surge simulation; we selected the top five provinces with the highest simulated storm surge. We applied boundary grids to the province shapefiles to create a catchment. Data with a grid resolution of 20 m $\times$ 20 m were used through the provided DTM data. The flood simulation runs smoothly if the storm surge's estimated peak discharge, Q_{peak}, divided by the grid element surface area, A_{grid}, does not exceed 3 m^3 s^{-1}. After considering the simulation time, we set the grid size to 20 m. Figure 3 shows a sample of inundation results, such as the maximum water surface depth and maximum flow depth, as shown in the FLO-2D model.

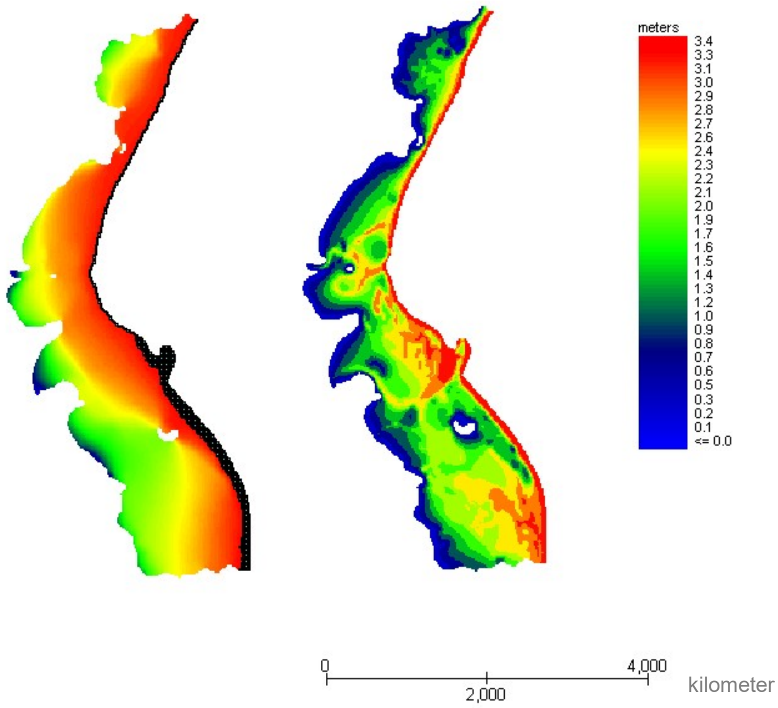

Figure 3. Maximum water surface depth and maximum flow depth in m as shown in the FLO2D model.

We used the calculated hydro-curve produced using the JMA storm surge model as input data for the FLO2D model, and then conducted inundation modeling.

3. Results and Discussion

3.1. Results of Storm Surge Coastal Inundation Model

We overlaid storm surge inundation results from the FLO-2D model on a satellite image for validation. Validation maps show an inundation color scale with ranges of 0.01–0.5 m (light yellow), 0.51–1.00 m (yellow), 1.01–1.50 m (red), 1.51–2.00 m (violet), and 2.01 m and above (blue). Validation points shown as blue circles observed flooding, and points represented as red circles experienced no inundation.

Figure 4 shows a comparison of observed inundation and simulated flooding for Tolosa, Leyte. Observed inundation and simulation results generally agreed. Flooding was observed (blue circles) in areas where the model had simulated storm surge inundation, and no flooding was observed (red circles) in areas with no simulated inundation. The same was true for the storm surge validation maps of El Nido, Palawan (Figure 5), Carles, Iloilo (Figure 6), and Marabut, Samar (Figure 7).

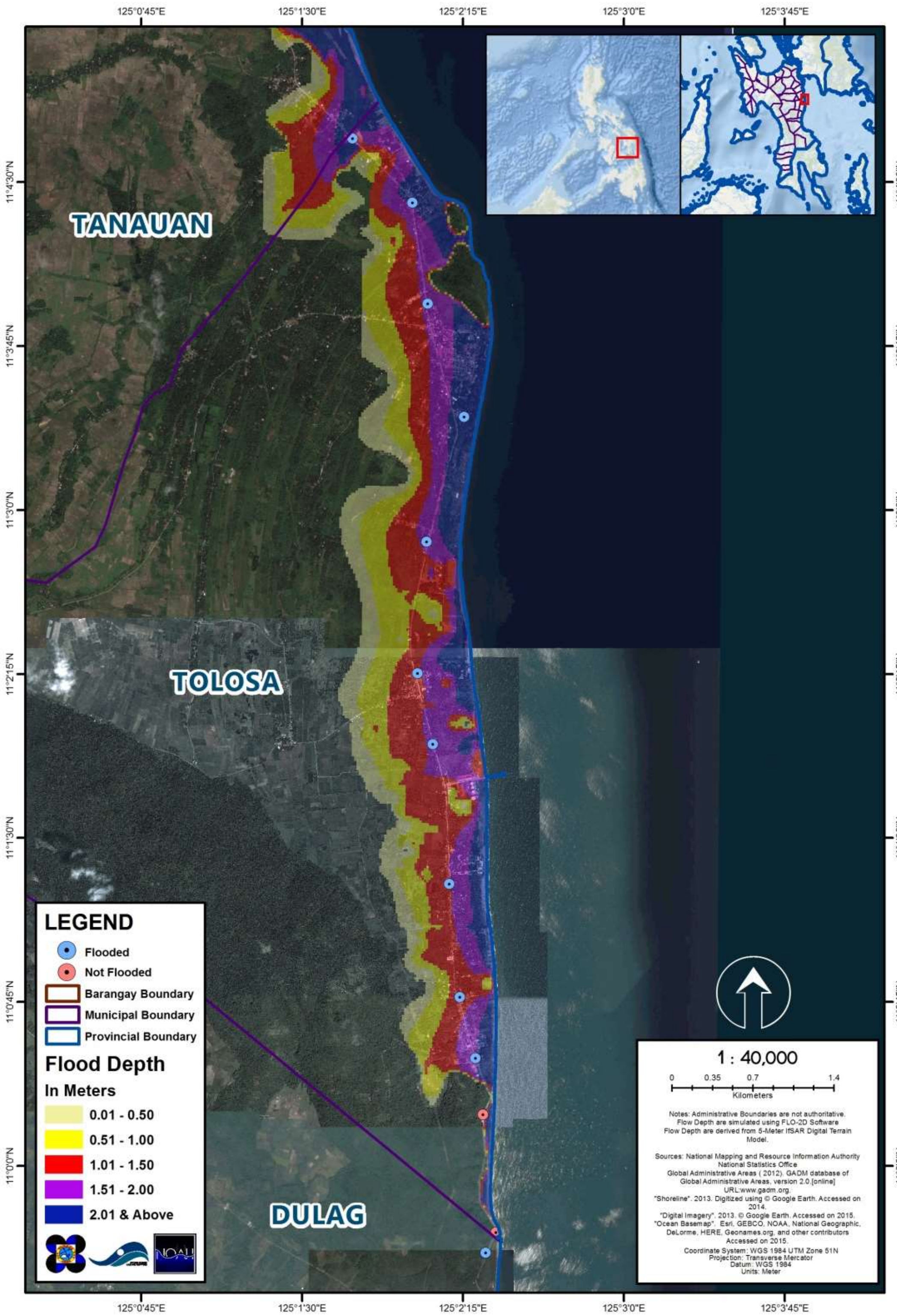

Figure 4. Storm surge inundation and validation points of Tanauan and Tolosa, Leyte. Validation points: blue circle (observed flooding) and red circle (no flooding).

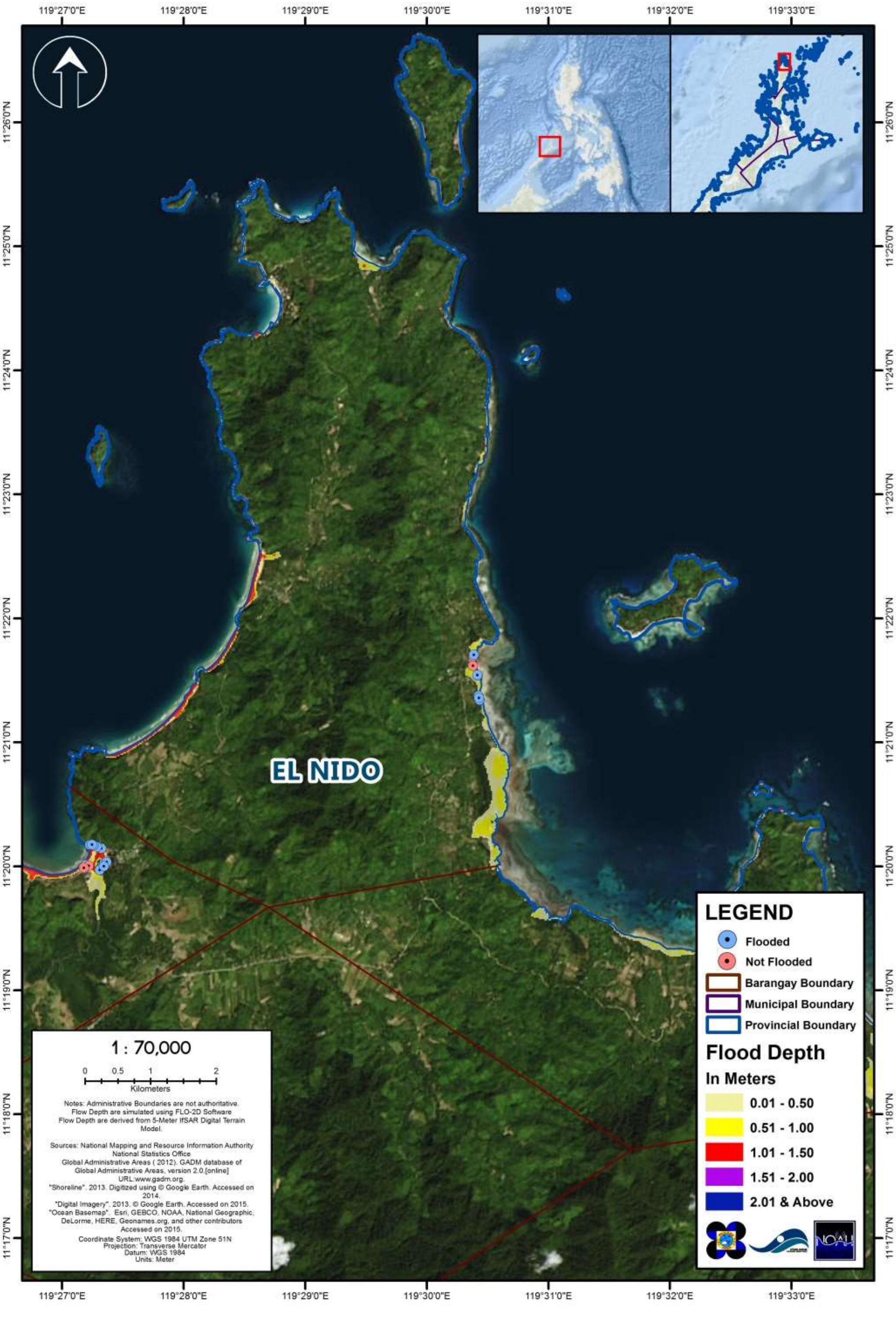

Figure 5. Storm surge inundation and validation points of El Nido, Palawan. Validation points: blue circle (observed flooding) and red circle (no flooding).

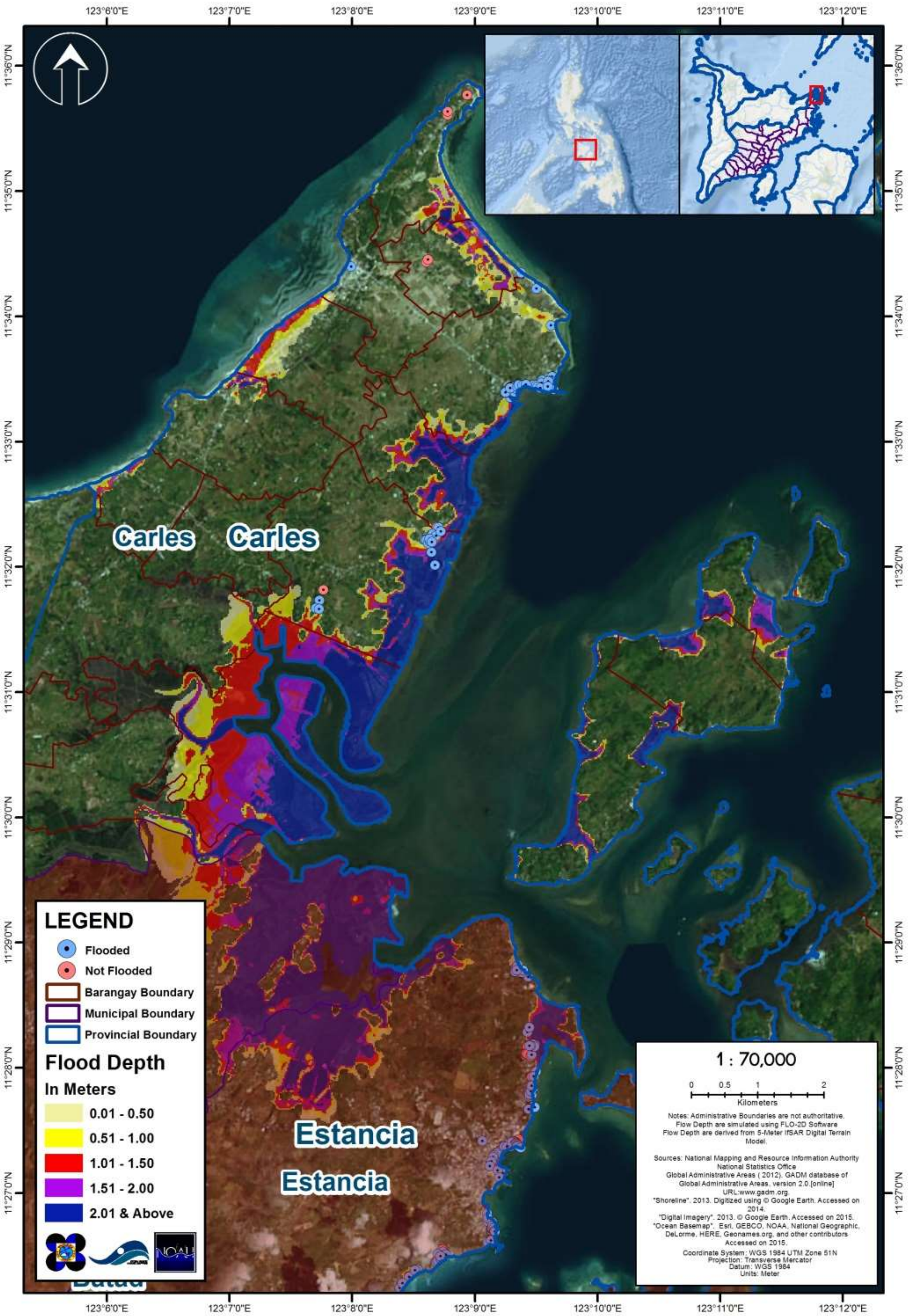

Figure 6. Storm surge inundation and validation points of Carles, Iloilo. Validation points: blue circle (observed flooding) and red circle (no flooding).

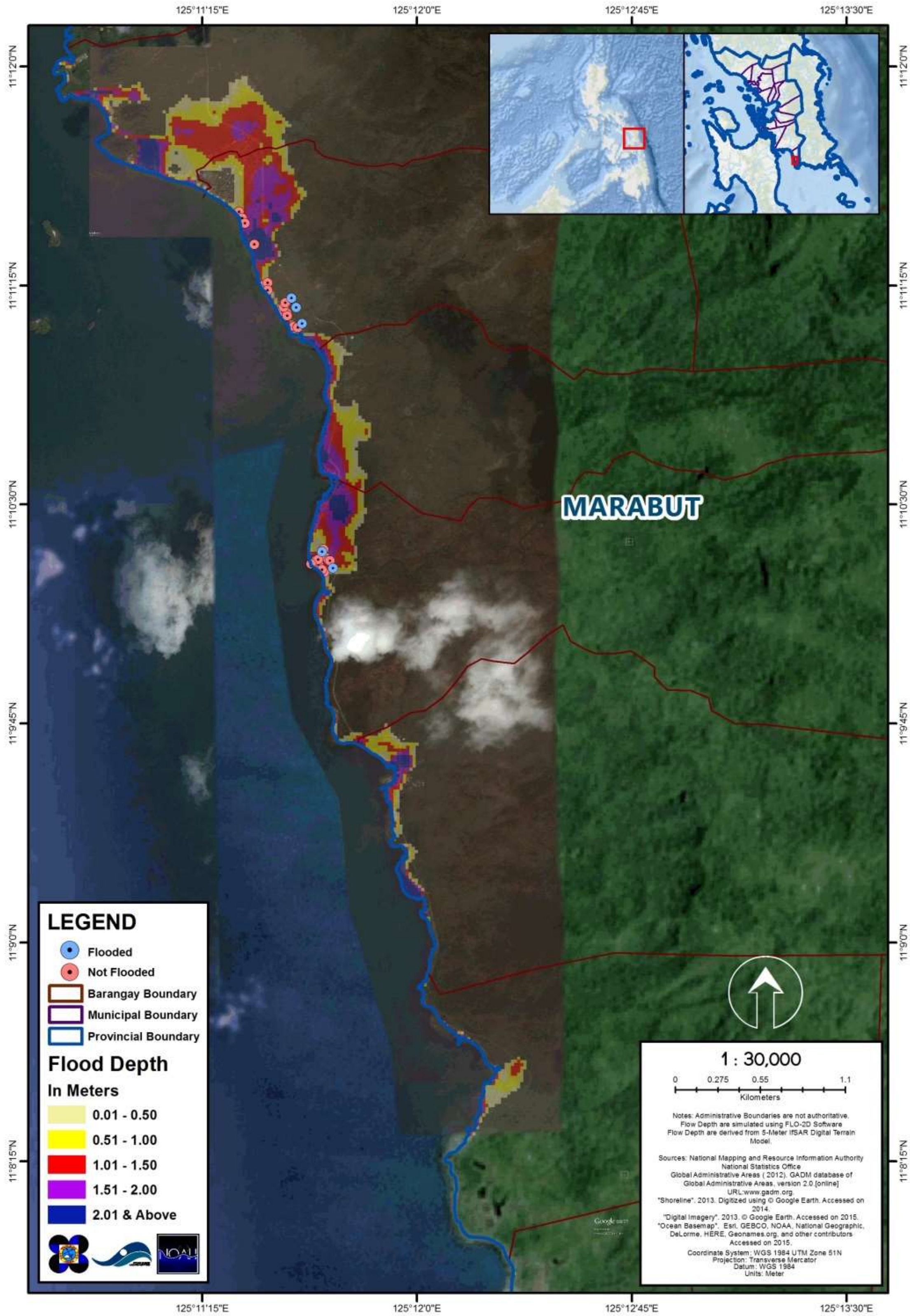

Figure 7. Storm surge inundation and validation points of Marabut, Samar. Validation points: blue circle (observed flooding) and red circle (no flooding).

However, the same cannot be said about the storm surge validation map of Guiuan, Eastern Samar (Figure 8). Flooding was observed at several validation points but showed no simulated storm surge, with the flooded area located 2000 km away from the coast (Figure 8). This is because the flooding that interviewees experienced may have been caused by rainfall, as Eastern Samar experienced about 120 mm of precipitation (Figure 8, lower left image) during Typhoon Haiyan.

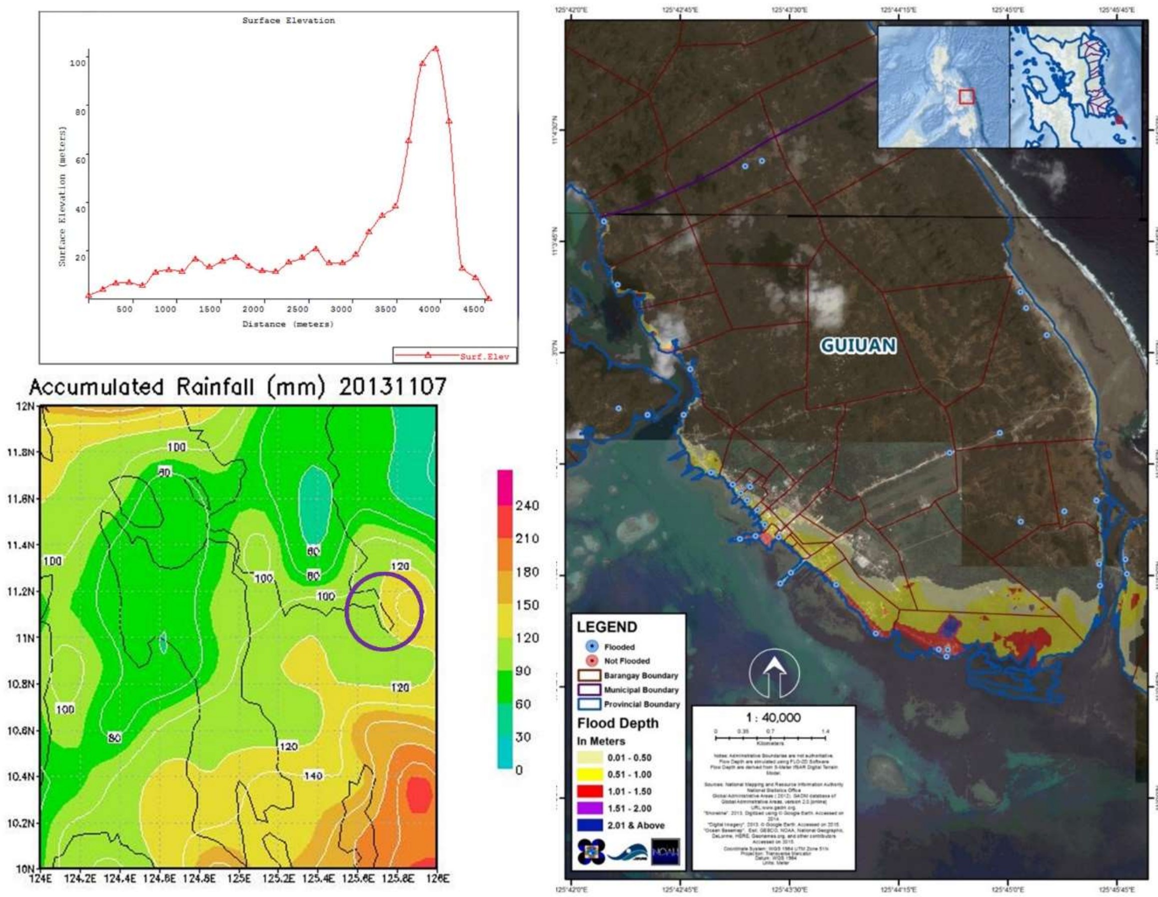

Figure 8. Storm surge inundation and validation points of Guiuan, Eastern Samar. The upper left figure shows the transect elevation for a cross-sectional transect (blue arrow) in the storm surge inundation map (right image). The lower left image shows accumulated rainfall during the event in mm/day, the area circled in purple is the area shown on the right panel.

3.2. Model Results Analysis

After establishing the reliability of the models that were used, it was necessary to determine why some coastal areas experiences worse storm surge compared to other areas. Based on the research by [22], Iloilo, Samar, Leyte, Palawan, and Eastern Samar provinces were among the top 25 Philippine coastal provinces most vulnerable to storm surge. A hypothetical track of a typhoon with Haiyan's wind strength would have a storm surge height as high as 7.45 m. This demonstrates that these provinces might possess geographical characteristics that make them more susceptible to damaging storm surges.

3.2.1. Effect of Elevation on Storm Surge Flow Depth

Varying storm surge flooding behavior can be seen in different elevation topographies. Figures 9 and 10 show cross-sectional and x height storm surge flooding in some of the simulated catchments. Figure 9 shows the effect of elevation on storm surge height, with lower elevation areas having greater storm surge height, as seen in the A to A′ and B to B′ transects. However, Figure 10 shows that coastal areas are not automatically vulnerable to storm surges if the area's elevation exceeds the maximum storm surge height.

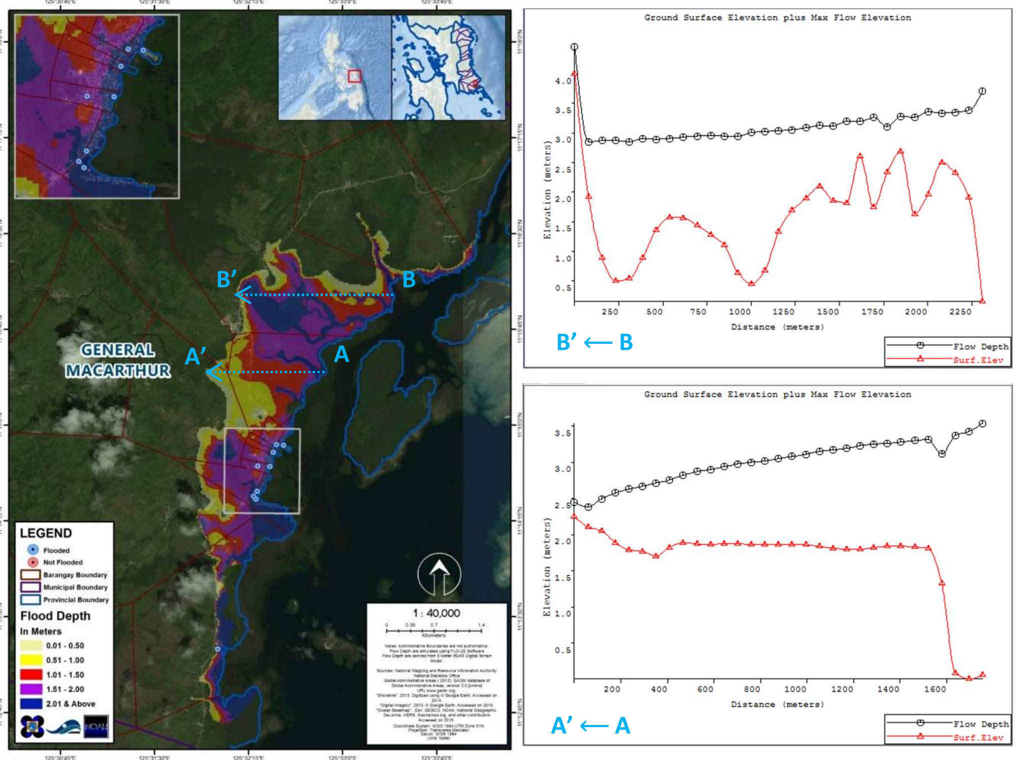

Figure 9. Storm surge inundation (left panel) and cross-sectional x height elevation (red line in right panel); storm surge flooding (black line) in terms of elevation for transects A to A′ and B to B′ (blue solid lines in the left panel,) showing effect of elevation on storm surge height.

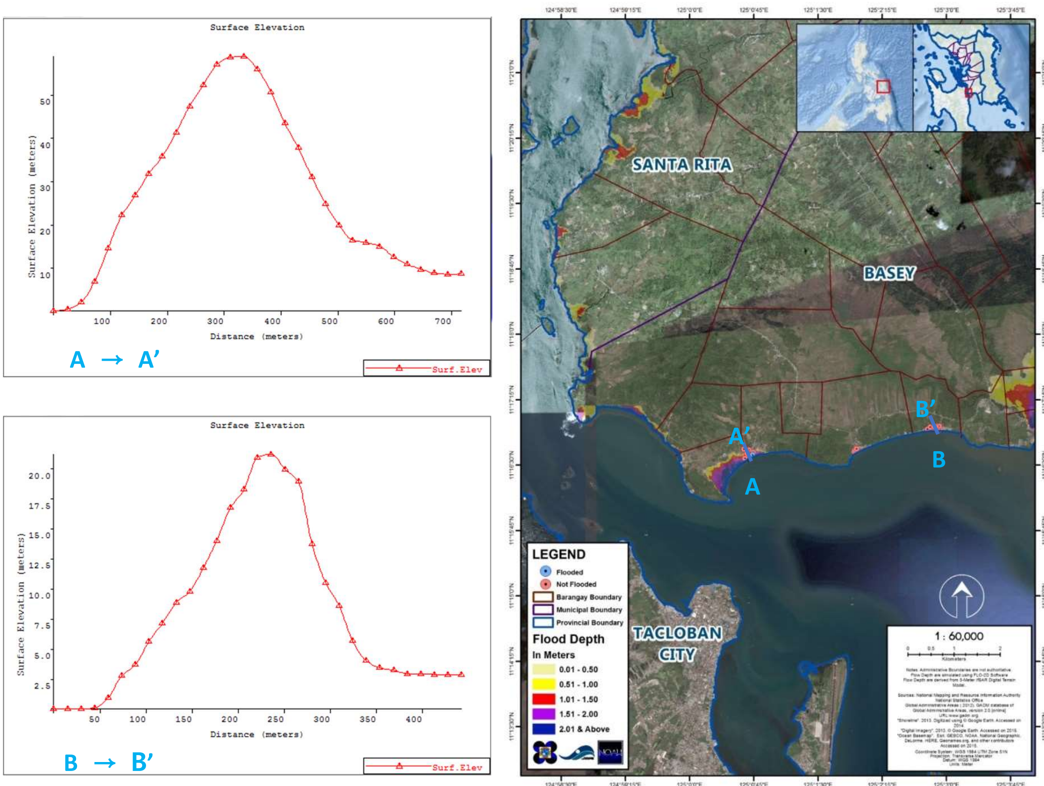

Figure 10. Storm surge inundation (right panel) and cross-sectional x height elevation with no flooding (red line in left panel) for transects A to A′ and B to B′ (blue solid lines in right panel), showing effect of elevation in storm surge height.

3.2.2. Effect of Elevation on Storm Surge Velocity

Determining flood velocity is also important for early warning efforts, because even low-level fast flowing floods are likely to cause significant damage. In addition to flow depth, the FLO-2D model can also map flow velocity, inundation duration, time to maximum depth, impact force, static pressure, specific energy, and hazard level.

Figure 11 shows a noticeable flow velocity increase that can be seen in the circled area. The circled area's elevation is shown in the boxed graph. The elevation graph shows that maximum flow velocity increased in the raised section in the middle, which can be explained by fluid behavior in that flow velocity is greater in areas that would cause fluids to compress (i.e., a corresponding velocity increase in smaller areas with a constant fluid volume).

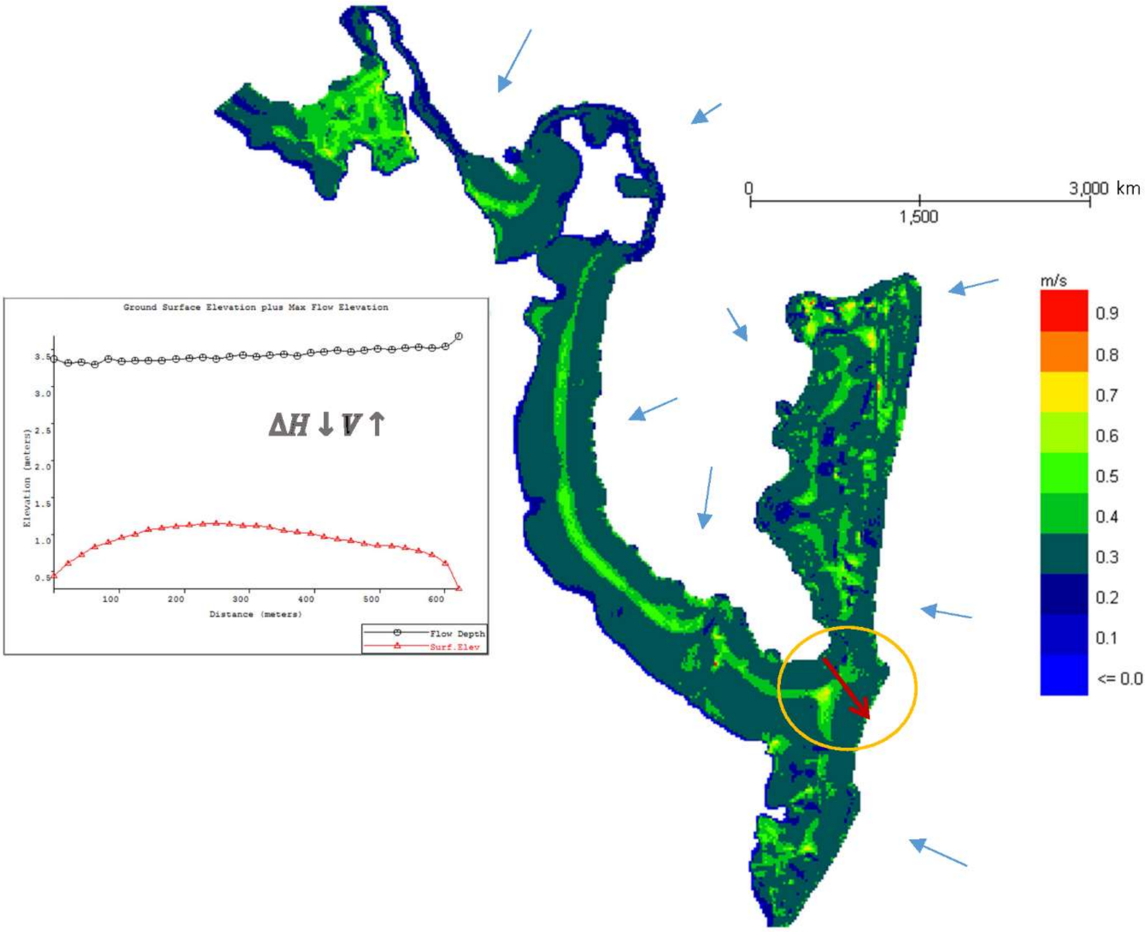

Figure 11. Map of maximum storm surge velocity (ms^{-1}). Storm surge inland flow direction is shown with blue arrows. Inset panel shows surface elevation versus storm surge height, with velocity of transect (red arrow) increasing as ΔH decreases.

3.2.3. Effect of Coastal Shape on Storm Surge Flow Depth

Coastal formation characteristics can also affect an incoming storm surge's extent and depth. Figures 12 and 13 show the coastal shape's effect on storm surge flow depth and extent. Storm surge flooding extents are farther away in coastal areas with concave coasts than those with straight-line coasts (circled areas), even at the same elevation. Fluid is more likely to be dispersed when hitting a convex coast, whereas fluid hitting a concave coast is likely to accumulate in the center, leading to a greater extent of flooding.

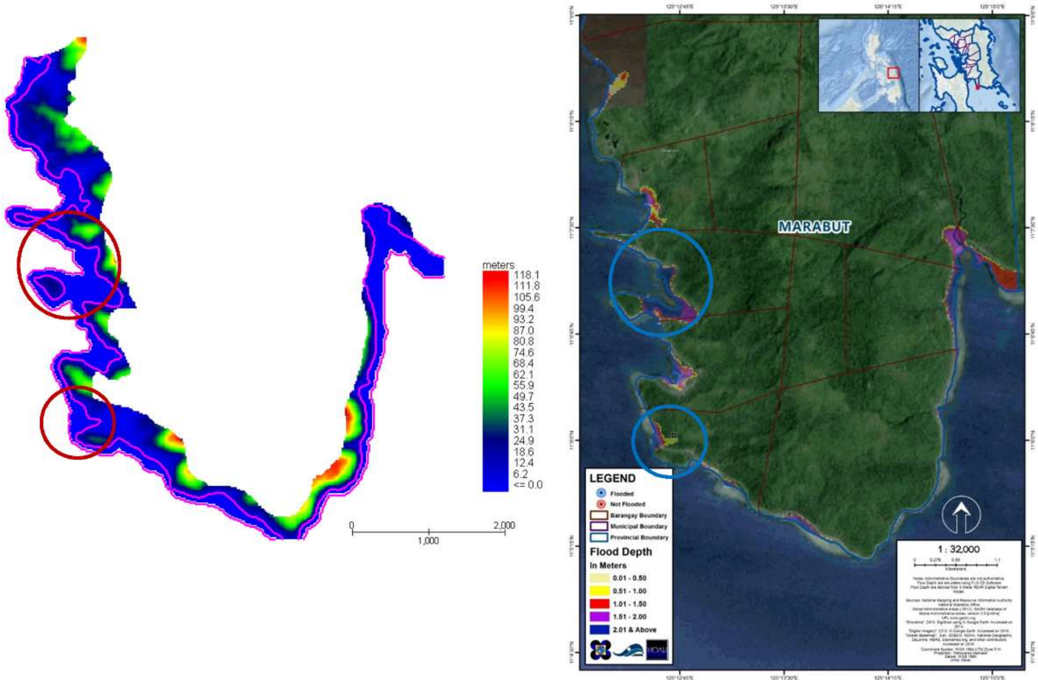

Figure 12. Effect of coastal shape on flow depth and extent in areas with the same elevation (Marabut, Samar). The right panel shows inland inundation, whereas the left panel shows the elevation contour (pink line is flooding extent), proving that the inundated regions (circled areas) are low-lying coasts.

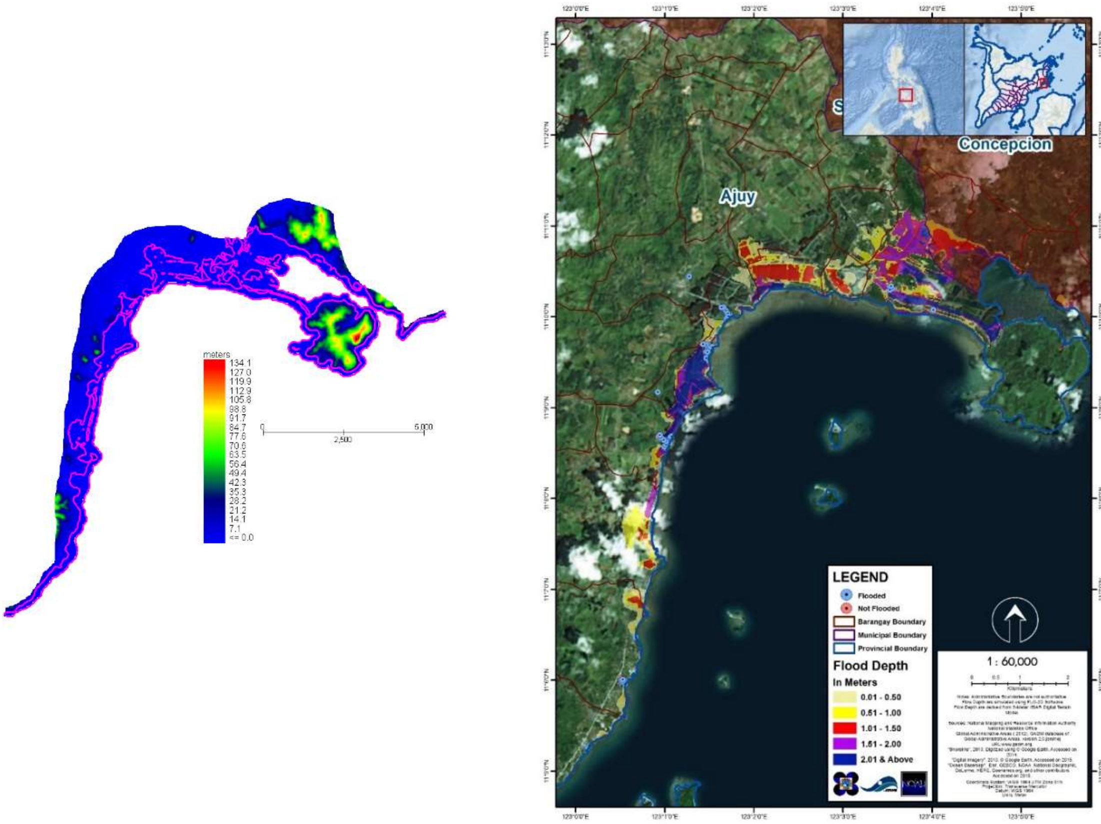

Figure 13. Effect of coastal shape on flow depth and extent in areas with the same elevation (Ajuy, Iloilo). The right panel shows inland inundation, whereas the left panel shows elevation contour (pink line is flooding extent), proving that inundated regions are low-lying coasts.

3.2.4. Effect of Coastal Shape on Storm Surge Velocity

We also found storm surge differed in response to the shape of the coast. Figure 14 shows velocity behavior differences in areas with dissimilar coastal characteristics and demonstrates that the maximum velocity increases in the center of catchments with equal distance from storm surge inflows. Vector velocity grids in the boxed areas of Figure 14 show uniform storm surge discharge from all directions, which then accumulate in the center. Thus, the flow velocity increases, because the fluid now has more momentum to flow in a single direction.

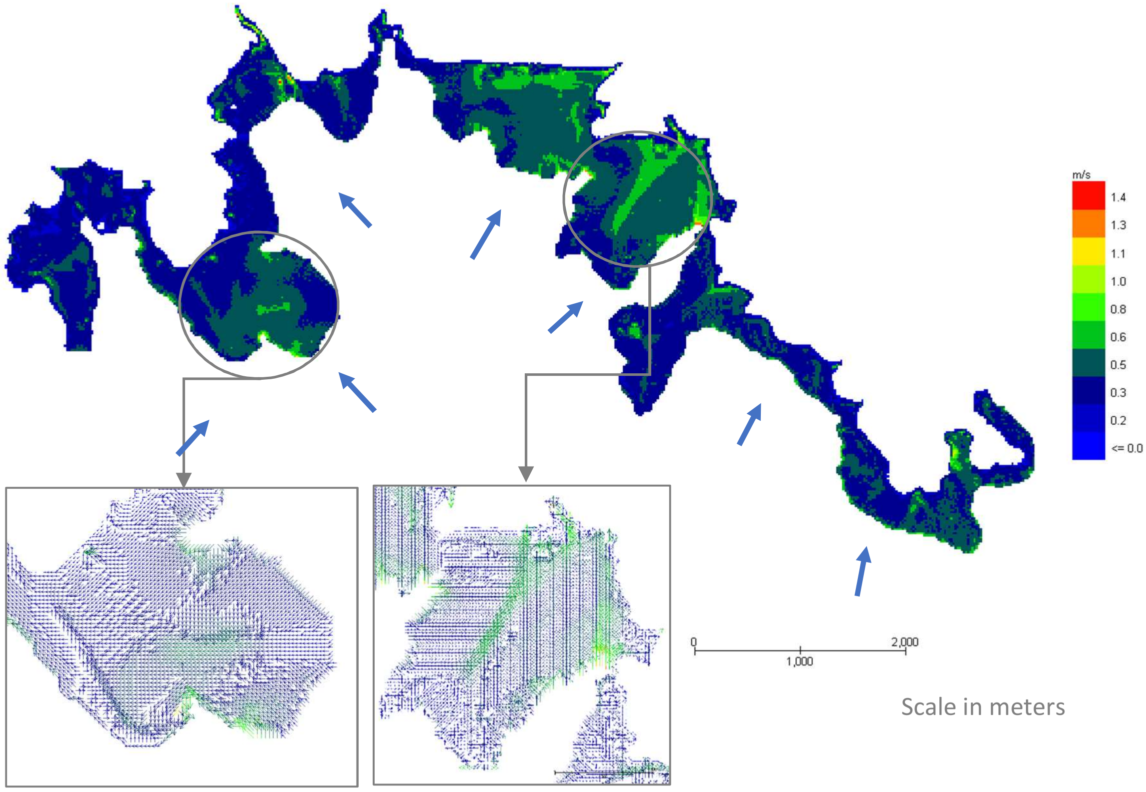

Figure 14. Maximum velocities (ms^{-1}) at constant elevation, blue arrows showing inland flow direction. Lower panels display zoomed-in regions showing directional velocity of flow, green and yellow areas having higher velocity flow compared with the blue ones.

3.2.5. Effect of Angle of Approach on Flow Depth

Differences in the typhoon's angle of approach to the coast can also affect the extent of storm surge. Figure 15 shows that extent of inundation was farther in areas that were directly hit by the typhoon. Typhoons that move onshore perpendicular to the coast tend to produce higher storm surges than those moving parallel to or at an oblique angle to the coast [23]. [24] also conducted research regarding the response in storm surge height to wind direction for cities exposed at the end of a long inlet, as compared to cities exposed in straight coastline. Changes in storm surge heights and extents were observed by simulating changes in the angle of directional wind. The same methodology was applied by [25] to this event, supporting the results that the orientation of coastal area relative to the typhoon's wind direction is a major factor in simulating expected storm surge.

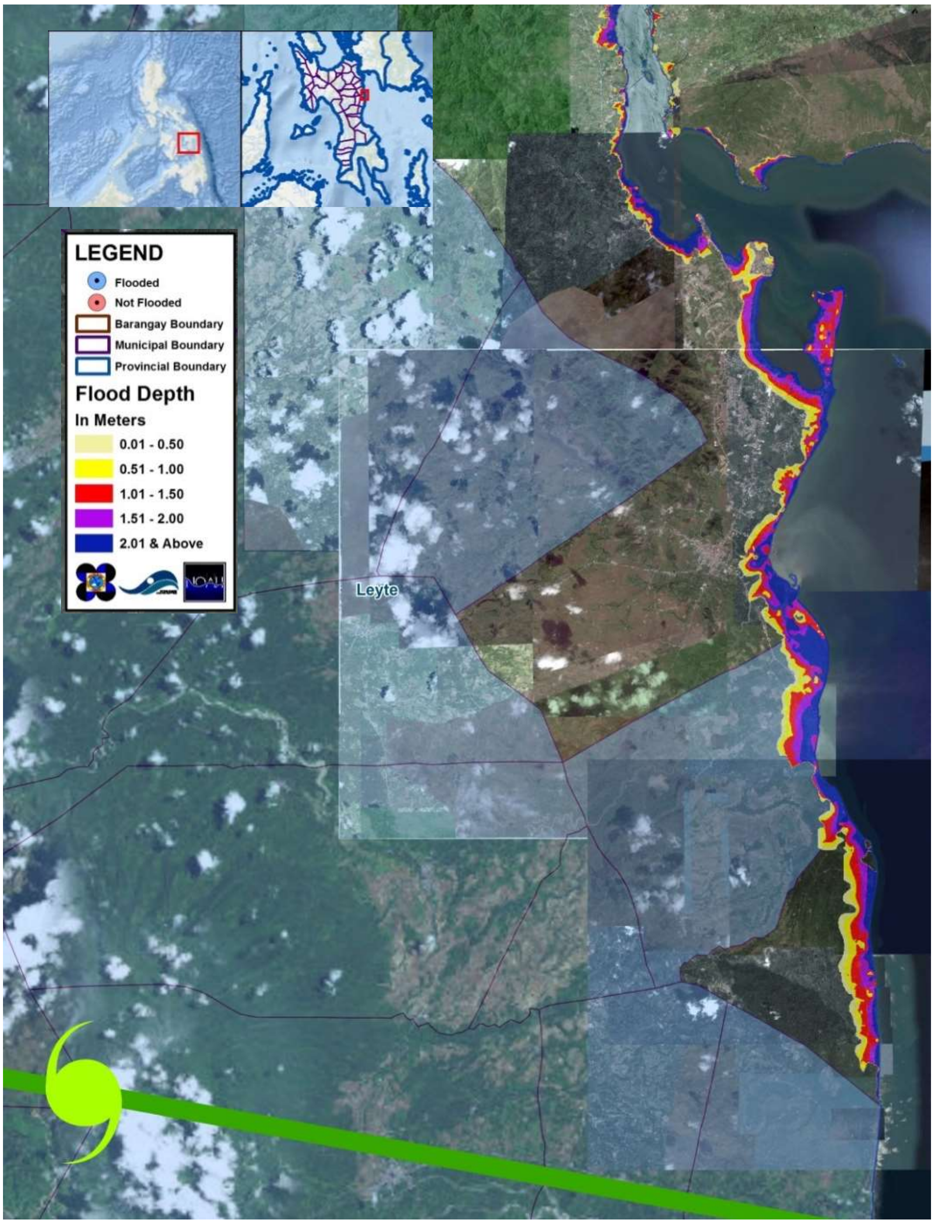

Figure 15. Effect of typhoon's approach angle on storm surge flow depth. The area delineated by the red box shows coasts directly perpendicular to the typhoon's wind direction, whereas the blue boxed area shows the coast that is parallel to the wind direction.

4. Conclusions

We simulated Typhoon Haiyan's storm surge height and inundation on the most affected coastal provinces in the Philippines, using the JMA storm surge model and the FLO-2D flood routing model, respectively. The reliability of the models used was proven through validation using actual storm surge records for Typhoon Haiyan. Note that we only conducted qualitative analysis for the effect of quantitative analysis, because of lack of validation data.

Storm surge model results identified Iloilo, Samar, Leyte, Palawan, and Eastern Samar provinces as having the greatest storm surge heights during Typhoon Haiyan, with the maximum storm surge height as high as 3.9 m. We subsequently used these province catchments for FLO-2D flood modeling.

We analyzed the aggravation of storm surge depth and extent in terms of the coast's topographical characteristics. Analysis shows significant effects of elevation, coastal shape, and inland approach angle on flood depth and storm surge velocity. The detailed findings are as follows:

- Flow depth analysis in terms of elevation indicated that deeper flooding events were experienced in areas with lower ground elevations (estuaries, low elevation sand lines), whereas coastal areas with higher elevations were not inundated even when the area was directly located on the coast.
- Flow velocity analysis in terms of elevation indicated that the maximum velocity increased in the center of catchments with higher elevation and equal distance from storm surge inflows; floods flowed faster in areas that would drive the fluid to compress.
- Flow depth analysis in terms of coastal shape indicated that some areas are flooded more than others, even with the same elevation, due to differences in coastal shape. This is due to the fact that fluid is more likely to be dispersed when hitting a convex coast, whereas fluid hitting a concave coast is likely to accumulate in the center, leading to a greater extent of flooding.
- Flow velocity analysis in terms of coastal shape revealed that in some regions with same level of elevation, flood velocity appeared to be faster in the central areas of catchment that had inflow parameters in all directions.
- Flow depth analysis in terms of a typhoon's angle of approach indicated that extents are farther in the areas that are directly hit by the typhoon; coastlines that are perpendicular to the to the typhoon's directional approach displayed a greater tendency to produce storm surges to a greater extent than those that are parallel to the coast.

Through these analyses, we can conclude that not all coastal areas are vulnerable to storm surges. Some regions may be more inundated than others depending on their physical inland characteristics, which can be used to improve early warning systems and long-term coastal urban planning.

Author Contributions: The simulations, field data comparison and writing research draft was done by L.D.; Conceptualization, model analysis and overall organization was done by S.L.; Analysis and final research writing were done by L.D. and S.L.

Acknowledgments: This research was supported by the APEC Climate Center. The models and the validation data used in this research were provided through the author's affiliation with the Philippine Nationwide Operational Assessment of Hazards (UP NOAH Center). The authors would like to acknowledge the contribution and support of the UP NOAH Center Team-Executive Director Mahar Lagmay and the Research and Development Chief Science Research Specialist John Kenneth Suarez. The authors would also like to express gratitude to the reviewers' insightful comments that had contributed to the further improvement of quality of this paper.

Conflicts of Interest: The authors declare no conflicts of interest.

References

1. National Disaster Risk Reduction and Management Council. NDRRMC Update: Final Report re Effects of Typhoon "Yolanda" (Haiyan). 2014. Available online: http://www.ndrrmc.gov.ph/attachments/article/1329/FINAL_REPORT_re_Effects_of_Typhoon_YOLANDA_HAIYAN_06-09NOV2013.pdf (accessed on 18 October 2018).
2. Lagmay, A.; Agaton, R.; Bahala, M.; Briones, J.; Cabacaba, K.; Caro, C.; Dasallas, L.; Gonzalo, L.; Ladiero, C.; Lapidez, J.; et al. Devastating storm surge of Typhoon Haiyan. *Int. J. Dis. Risk Reduct.* **2015**, *11*, 1–12. [CrossRef]
3. Mercado, A. On the Use of NOAA's Storm Surge Model, SLOSH, in Managing Coastal Hazards—The Experience in Puerto Rico. *Nat. Hazards* **1994**, *10*, 235–246. [CrossRef]
4. Li, J.; Nie, B. Storm surge prediction: Present status and future challenges. *Procedia IUTAM* **2017**, *25*, 3–9. [CrossRef]
5. Elsaesser, B.; Bell, A.; Shannon, N.; Robinson, C. Storm surge hind- and forecasting using Mike21FM—Simulation of surges around the Irish Coast. In Proceedings of the DHI International User Conference, Copenhagen, Denmark, 6–8 September 2010.
6. Veeramony, J.; Condon, A.; Linzell, R.; Watson, K. *Validation of Delft3D as a Coastal Surge and Inundation Prediction System*; Naval Research Laboratory Stennis Space Center: Hancock County, MA, USA, 2016.
7. Higaki, M.; Hayashibara, H.; Nozaki, F. Outline of the Storm Surge Prediction Model at the Japan Meteorological Agency. *RSMC Tokyo-Typhoon Cent. Tech. Rev.* **2009**, *11*, 25–38.

8. Nakamura, R.; Shibayama, T. Ensemble forecast of extreme storm surge: A case study of 2013 Typhoon Haiyan. *Coast. Eng. Proc.* **2017**, *1*, 10. [CrossRef]
9. Lee, H.; Lim, K. Storm surge and storm waves modeling due to Typhoon Haiyan in November 2013 with improved dynamic meteorological conditions. *Procedia Eng.* **2015**, *116*, 699–706. [CrossRef]
10. May, S.; Engel, M.; Brill, D.; Cuadra, C.; Lagmay, A.; Santiago, J.; Suarez, J.; Reyes, M.; Brucker, H. Block and boulder transport in Eastern Samar (Philippines) during Supertyphoon Haiyan. *Earth Surf. Dyn. Discuss.* **2015**, *3*, 739–771. [CrossRef]
11. Soria, J.; Switzer, A.; Pilarczyk, J.; Siringan, F.; Khan, N.; Fritz, H. Typhoon Haiyan overwash sediments from Leyte Gulf coastlines show local spatial variations with hybrid storm and tsunami signatures. *Sediment. Geol.* **2017**, *358*, 121–138. [CrossRef]
12. Kim, K. Typhoon storm surge simulation for Typhoon Haiyan. *J. Int. Dev. Coop.* **2015**, *21*, 17–25.
13. Soria, J.; Switzer, A.; Villanoy, C.; Fritz, H.; Bilgera, P.; Cabrera, O.; Siringan, F.; Yacat-Sta. Maria, Y.; Ramos, R.; Fernandez, I. Repeat storm surge disasters of Typhoon Haiyan and its 1897 predecessor in the Philippines. *Am. Meteorol. Soc.* **2016**, *97*, 31–48. [CrossRef]
14. Takagi, H.; Mikami, T.; Esteban, M.; Matsumaru, R. Track Analysis, Simulation and Field Survey of the 2013 Typhoon Haiyan. *J. Flood Risk Manag.* **2014**, *10*, 42–52. [CrossRef]
15. Mori, N.; Kato, M.; Kim, S.; Mase, H.; Shibutani, Y.; Takemi, T.; Tsuboki, K.; Yasuda, T. Local amplification of storm surge by Super Typhoon Haiyan in Leyte Gulf. *Geophys. Res. Lett.* **2014**, *41*, 5106–5113. [CrossRef] [PubMed]
16. Bricker, J.; Takagi, H.; Mas, E.; Kure, S.; Adriano, B.; Yi, C.; Roeber, V. Spatial variation of damage due to storm surge and waves during Typhoon Haiyan in the Philippines. *J. Jpn. Soc. Civil Eng.* **2014**, *70*, 231–235. [CrossRef]
17. Japan Meteorological Agency. RSMC Best Track Data. 2013. Available online: http://www.jma.go.jp/jma/jma-eng/jma-center/rsmc-hp-pub-eg/Besttracks/bst2015.txt (accessed on 2 June 2016).
18. Smith, S.D.; Banke, E.G. Variation of the sea surface drag coefficient with wind speed. *Quart. J. R. Meteorol. Soc.* **1975**, *101*, 665–673. [CrossRef]
19. Frank, W.M. Composite analysis of the core of a mature hurricane. *Mon. Weather Rev.* **1984**, *112*, 2401–2420. [CrossRef]
20. Hasegawa, H.; Kohno, N.; Hayashibara, H. JMA's Storm Surge Prediction for the WMO Storm Surge Watch Scheme (SSWS). *RSMC Tokyo-Typhoon Cent. Tech. Rev.* **2012**, *14*, 12.
21. FLO-2D Software, Inc. *FLO-2D Reference Manual 2009 | Flood | Fluid Dynamics*; FLO-2D Software, Inc.: Nutrioso, AZ, USA, 2017.
22. Lapidez, J.P.; Tablazon, J.; Dasallas, L.; Gonzalo, L.A.; Cabacaba, K.M.; Ramos, M.M.A.; Suarez, J.K.; Santiago, J.; Lagmay, A.M.F.; Malano, V. Identification of storm surge vulnerable areas in the Philippines through the simulation of Typhoon-induced storm surge levels over historical storm tracks. *Nat. Hazards Earth Syst. Sci.* **2015**, *3*, 919–939. [CrossRef]
23. National Hurricane Center. Storm Surge Overview. 2016. Available online: http://www.nhc.noaa.gov/surge/surge_intro.pdf (accessed on 15 July 2016).
24. Drews, C. Directional Storm Surge in Enclosed Seas: The Red Sea, the Adriatic, and Venice. *J. Mar. Sci. Eng.* **2015**, *3*, 356–367. [CrossRef]
25. Drews, C.; Galarneau, T. Directional Analysis of the Storm Surge from Hurricane Sandy 2012, with Application to Charleston, New Orleans, and the Philippines. *PLoS ONE* **2015**, *10*, e0122113. [CrossRef] [PubMed]